Available online at www.sciencedirect.com
SCIENCE DIRECT®
Journal of Magnetic Resonance 161 (2003) 191–197
JMR Journal of Magnetic Resonance
www.elsevier.com/locate/jmr

Solid state ^{33}S NMR of inorganic sulfides

Todd A. Wagler,[a] William A. Daunch,[a] Peter L. Rinaldi,[a,*] and Allen R. Palmer[b]

[a] *Department of Chemistry, Knight Chemical Laboratory, The University of Akron, 190 E. Buchtel Commons, Akron, OH 44325-3601, USA*
[b] *Varian, Inc., 2607 Midpoint Drive, Fort Collins, CO 80525, USA*

Received 3 September 2002; revised 28 January 2003

Abstract

Solid state ^{33}S NMR spectra of a variety of inorganic sulfides have been obtained at magnetic field strengths of 4.7 and 17.6 T. Spectra acquired with magic angle spinning show considerable improvements in sensitivity and resolution when compared with static spectra. Multiple factors are considered when analyzing the spectral line widths, including; magnetic field inhomogeneity, dipolar coupling, chemical shift anisotropy, chemical shift dispersion (CSD), T_2 relaxation, and quadrupolar coupling. Quadrupolar coupling was expected to be the dominant line broadening mechanism. However, for most of the samples CSD was the prevailing line broadening mechanism. Thus, for many of the metal sulfides studied at a high magnetic field strength, the line widths were actually larger than those observed in the spectra at low field. This is atypical in solid state ^{33}S NMR. Solid state ^{33}S spin–lattice (T_1) and spin–spin (T_2) relaxation rates were measured for the first time and are discussed. This information will be useful in future efforts to use ^{33}S NMR in the compositional and structural analysis of sulfur containing materials.

1. Introduction

Sulfur chemistry is important in many biological, geological, and chemical processes. ^{33}S, the only isotope of sulfur detectable by NMR, also happens to be among the first NMR-active nuclei to be observed [1]. However, ^{33}S NMR has not been used extensively as a tool in understanding sulfur chemistry. Fewer than 200 scientific papers have been published in a span of almost 50 years. Four excellent reviews have been published on ^{33}S NMR since 1970; however, much of the reviewed information has focused on ^{33}S NMR in solution [2–5].

There are good reasons why so little ^{33}S NMR work has been published. ^{33}S has a small gyromagnetic ratio (1/13 that of ^{1}H) and a low natural abundance (0.76%), making it among the most difficult nuclei to study by NMR. Its receptivity, a measure of the absolute signal strength of a fixed number of nuclei, is 1.7×10^{-5} relative to that of ^{1}H and 9.72×10^{-2} relative to that of ^{13}C [6]. Furthermore, unlike the more commonly studied ^{1}H and ^{13}C nuclei, ^{33}S is a quadrupolar nucleus with a nuclear spin $I = 3/2$ and has a relatively large quadrupole moment ($Q = -6.4 \times 10^{-28}\,\mathrm{m}^2$). The large quadrupole moment results in rapid T_2 relaxation leading to extremely broad lines in chemical species having unsymmetrical sulfur environments.

Even with these inherent difficulties, there are very compelling reasons to use ^{33}S NMR. Significant chemical structure information can be obtained, by directly observing ^{33}S. Its chemical shift range exceeds 800 ppm , which is approximately four times that of ^{13}C and nearly 16 times that of ^{1}H. Additionally, because sulfur is often directly involved in many of the chemical transformations of interest, its NMR properties are more sensitive than the NMR properties of nuclei such as ^{1}H and ^{13}C which are only indirectly affected.

With three formal oxidation states, the sulfur atom can form two single bonds (S^{II}), or can be hypervalent (S^{IV} and S^{VI}), forming four- and six-coordinate structures. Most of the solution NMR studies have been done on S^{IV} and S^{VI} species, which exist in environments with high electronic symmetry around the S atom. For all compounds but those with the most symmetric electronic environments around sulfur, the relatively large quadrupole moment of ^{33}S leads to rapid T_2 relaxation. This produces broad spectral lines that very

* Corresponding author. Fax: 1-330-972-5256.
E-mail address: PeterRinaldi@uakron.edu (P.L. Rinaldi).

1090-7807/03/$ - see front matter © 2003 Elsevier Science (USA). All rights reserved.
doi:10.1016/S1090-7807(03)00046-6

often obscure the resolution of separate resonances from distinct sulfur species.

In the solid state, the outer $(-(3/2) \leftrightarrow -(1/2)$ and $+(1/2) \leftrightarrow +(3/2))$ spectral transitions are usually broadened beyond detection by quadrupolar interactions or are so small that they are below the noise floor of the spectrum. However, the central $(-(1/2) \leftrightarrow +(1/2))$ transition, to a first approximation, is unaffected by these same interactions and can produce a relatively narrow resonance. In cases where the quadrupolar interaction is comparable to the resonance frequency (e.g., in unsymmetrical structures), second order quadrupolar effects can lead to significant broadening of the central transition. Considering that the spectral line width is inversely proportional to the strength of the applied magnetic field, this broadening can be reduced by using a stronger magnetic field [7].

Until recently, it has been exceedingly difficult to extract information from the NMR spectra of quadrupolar nuclei. Fortunately, higher magnetic field strengths and a variety of new experimental techniques can now be used to average the effect of quadrupolar broadening, and improve both sensitivity and resolution. Line narrowing can be attained through partial averaging of the second order quadrupolar interaction using high speed sample rotation at the "magic angle," $\theta = 54.7°$. Theoretical investigations of the quadrupolar spin interaction tensors have shown that complete averaging can be achieved by mechanical means (e.g., dynamic angle spinning [8–11] and double rotation [12,13]), or by pulsed NMR techniques like multiple quantum excitation [14,15].

Although few publications have appeared in the scientific literature describing applications of solid state ^{33}S NMR, the most comprehensive study to date was published in 1986 [16]. In that work, which was performed with hardware available at the time, the authors examined chemical shifts, line widths, and second order quadrupolar broadening effects on the static line shapes of the central $(-(1/2) \leftrightarrow +(1/2))$ transition of a number of sulfur containing inorganic compounds. Fifteen years have elapsed since this initial publication with very little new work appearing in the literature [17,18]. To determine the degree of resolution and sensitivity enhancement achievable with current instrumental capabilities, this paper compares solid state ^{33}S spectra of a variety of inorganic sulfide compounds obtained at 4.7, 11.7, and 17.6 T.

2. Experimental

A variety of sulfur containing inorganic compounds were obtained from commercial sources and used as received. Table 1 provides additional details regarding these samples. ^{33}S NMR data were collected on Varian Unity^{plus} 200 and 750 MHz NMR spectrometers operating at 4.7 and 17.6 T, respectively. Samples were packed as powders into silicon nitride or zirconia ceramic rotors and sealed with Vespel or Kel-F end caps. All samples underwent MAS with rates ranging from 0 to 6 kHz. A Doty Scientific wide bore broadband solid state MAS probe, optimized for observing ^{13}C at 4.7 T, was tuned to the lower ^{33}S resonance frequency by adding additional capacitance to the probes X channel tuning circuit. A Varian/Chemagnetics T3 double-channel probe, optimized for observing ^{33}S, was used with the Unity^{plus} 750 MHz spectrometer.

Table 1
Inorganic sulfide compounds studied

Compound	Supplier	Crystal lattice structure (Ref.)	Purity (%)
Li_2S	Aldrich	Cubic [30–32]	98
Na_2S	Aldrich	Cubic [31–33]	97
MgS	Pfaltz and Bauer	Cubic [34,35]	99.9
CaS	Aldrich	Cubic [34–36]	99.9
ZnS	Aldrich	Cubic/hexagonal [37–41]	99.99
SrS	Alfa	Cubic [34–36,42]	99.9
PbS	Aldrich	Cubic [43–46]	99.9
BaS	Alfa	Cubic [35,36,47]	99.7

Magnetic field homogeneity was adjusted by shimming on the deuterium or proton signal from 99% D_2O. At 4.7 and 17.6 T the ^1H line widths at half height from the residual H_2O were 4 and 12 Hz, respectively. The B_0 field inhomogeneity contribution to the ^{33}S line width was estimated to be $\leqslant 1$ Hz. Chemical shift referencing and 90° pulse widths were determined using primary and secondary ^{33}S standards. ^{33}S signals were referenced relative to external 1 M aqueous Cs_2SO_4 (333 ppm). The 90° pulse widths were determined using either 1 M aqueous Cs_2SO_4 or solid CaS (cubic symmetry), both samples gave the same result. Typical 90° (liquid) pulse width values were 5 and 8 μs at 17.6 and 4.7 T, respectively.

A one-pulse experiment was used at 17.6 T to obtain spectra for chemical shift and line width measurements. Because a baseline roll from acoustic probe ringing was observed at low field, the ring down elimination (RIDE) pulse sequence [4], was used to acquire spectra at 4.7 T for those samples that gave broad resonances. Fortunately, acoustic probe ringing was significantly reduced at 17.6 T, because of the higher resonance frequency, optimized design of the probe circuit, and optimized selection of probe materials. After acquiring the data with a simple one-pulse experiment, distortions at the beginning of the FID never persisted for more than the first two to six points. Since many of the FIDs lasted for hundreds or thousands of points, linear back prediction was sufficient to correct the distortion [19]. Spin lattice relaxation (T_1) measurements were obtained using the inversion recovery sequence (delay–π–τ–π/2—acquire), and spin–spin relaxation measurements (T_2) were

obtained using the Carr–Purcell–Meiboom–Gill (CPMG) sequence (delay–$\pi/2$–$[\tau$–π–$\tau]_n$–acquire).

The solid state ^{33}S NMR spectra of the eight inorganic sulfides studied were acquired at 17.6 T using the following parameters: (a) Li_2S, 10° pulse, 500 ms relaxation delay, 164 ms acquisition time, 3072 scans with 40 Hz line broadening, experiment time was 40 min; (b) Na_2S, 10° pulse, 500 ms relaxation delay, 164 ms acquisition time, 1536 scans with 20 Hz line broadening, experiment time was 20 min; (c) MgS, 10° pulse, 500 ms relaxation delay, 164 ms acquisition time, 225 k scans with 10 Hz line broadening, experiment time was 48 h; (d) CaS, 10° pulse, 200 ms relaxation delay, 200 ms acquisition time, 768 scans with 10 Hz line broadening, experiment time was 10 min; (e) ZnS, 10° pulse, 500 ms relaxation delay, 33 ms acquisition time, 278 k scans with 40 Hz line broadening, experiment time was 42 h; (f) SrS, 10° pulse, 200 ms relaxation delay, 164 ms acquisition time, 131 k scans with 20 Hz line broadening, experiment time was 13.5 h; (g) PbS, 45° pulse, 500 ms relaxation delay, 20 ms acquisition time, 16 k scans with 100 Hz line broadening, experiment time was 2.5 h. (h) BaS, 10° pulse, 100 ms relaxation delay, 82 ms acquisition time, 300 k scans with 10 Hz line broadening, experiment time was 16 h.

Spectral simulations were carried out in an attempt to determine the relative magnitude of the quadrupole coupling constant (QCC). Simulations were performed on a Sun Ultra Sparc workstation using the Varian STARS solid line shape simulation package [20–22].

3. Results and discussion

Typically, in solid state ^{33}S NMR, the QCC plays a dominant role in defining the spectral line width. At first, it was surprising to observe such narrow spectral lines in the ^{33}S spectra. Similar spectra of inorganic sulfates showed much larger line widths [23]. However, the QCC is unusually small in these compounds due to the high degree of symmetry around sulfur. Fig. 1 shows that the ^{33}S line widths are relatively narrow ($\leqslant 340$ Hz for the MAS spectra) and that there are no observable second order quadrupole splittings of the central transition in the spectra of the metal sulfides studied in this work. Based on comparisons with simulated spectra at 57.5 MHz (17.6 T) with various QCCs and asymmetry parameters (CSA set to 0 ppm), the QCC is estimated to be $\leqslant 0.5$ MHz for all of the inorganic sulfides studied. This is consistent with the highly symmetric electronic environment for sulfur in these compounds (see Table 1).

Several factors influence the spectral line width including; quadrupolar coupling, dipolar coupling, magnetic field inhomogeneity, CSA, CSD, and T_2 relaxation. In addition, the spectral line width is dependent on whether the experiment was run under static or MAS conditions. MAS can reduce or eliminate the contributions to the resonance line width from dipolar coupling, magnetic field inhomogeneity, and CSA. Furthermore, MAS can reduce the line width due to quadrupolar effects by a factor of 2.57 [24]. The quadrupolar coupling's contribution to the spectral line width is a function of the QCC and the magnetic field strength, and is of the order of the following factor [24]:

$$A = \frac{\mathrm{QCC}^2}{\upsilon_z} \cdot C_I, \tag{1}$$

where $C_I = 3/64$ for $I = 3/2$ and $\upsilon_z = \gamma B_0/2\pi$. Thus, increasing the field strength should result in a proportional decrease in line width if quadrupolar coupling is the primary contributor.

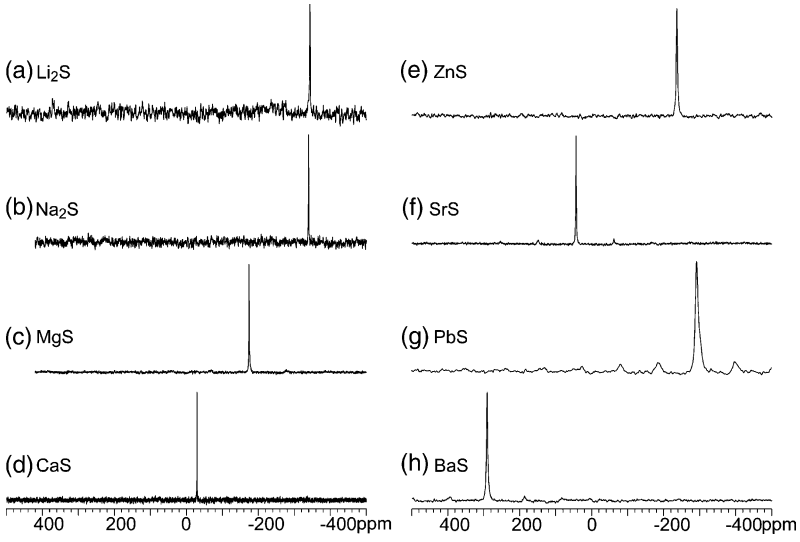

Fig. 1. Solid-state ^{33}S NMR spectra obtained at 57.5 MHz (17.6 T, 750 MHz ^{1}H resonance frequency). The liquid 90° pulse width was 5.5 μs. See text for details.

Dipolar coupling is dependent on the internuclear distance and the gyromagnetic ratios ($\gamma_I\gamma_S\hbar/r^3$) of the interacting nuclei. Most of the NMR active nuclei under consideration have a small gyromagnetic ratio. Only ^{7}Li, ^{23}Na and ^{207}Pb have relatively large values. The gyromagnetic ratios of ^{7}Li, ^{23}Na, and ^{207}Pb are 10.4×10^7 rad/T s, 7.1×10^7 rad/T s, and 5.6×10^7 rad/T s, respectively. However, because ^{33}S has a gyromagnetic ratio of 2.0534×10^7 rad/T s, the dipolar couplings are expected to be small and are effectively averaged to zero by MAS, even at modest spin rates of a few kHz. Magnetic field inhomogeneity was also found to be small, and contributes $\leqslant 1$ Hz to the width of the ^{33}S resonances. Spinning at frequencies greater than the static line width will eliminate broadening from CSA, dipolar coupling, and first order quadrupole coupling. Therefore, second order effects in the quadrupole coupling, T_2 relaxation, and CSD (from variations in sample morphology) must be the dominant factors influencing line width. The line width contribution from CSD is proportional to the magnetic field strength [25]. Thus, a 3.75-fold increase in field strength will result in a corresponding increase in CSD contributions to the line width.

Table 2 summarizes the line widths measured in this work and for which solid state ^{33}S NMR data have appeared in the literature [16]. A 20-fold reduction in line width was observed in the MAS spectra of Li_2S when compared with literature values reported for static samples. In some cases (e.g., Na_2S, MgS, and ZnS), approximately an order of magnitude reduction in line width was achieved. The MAS spectra of CaS, SrS, PbS, and BaS acquired at 4.7 T show approximately a 4-fold reduction in line width when compared to non-spinning literature values. The decrease in line width between the static and MAS spectra, even at low fields, shows that CSA and, to a smaller extent, dipolar coupling are the largest contributors to line width in the static spectra. Examination of the MAS spectra at 4.7 and 17.6 T shows that the line widths increase with increasing field strength for most of the sulfides studied. This shows that CSD is a dominant line broadening mechanism for the MAS spectra of these inorganic sulfides. Specifically, the effects of CSD are quite obvious in the line widths measured in the spectra of PbS. This is consistent with results of Neue et al. where they contend that small concentrations of lattice defects are responsible for the large broadening of the ^{207}Pb resonance in PbS [26]. ZnS is the only compound that shows significant broadening from second order quadrupolar coupling at low field. In the literature it is reported that ZnS can crystallize in cubic and/or hexagonal forms (see Table 1). Almost a 3-fold reduction in line width is observed in the MAS spectra when the field strength is increased from 4.7 to 17.6 T.

Table 3 shows the chemical shifts, T_1, and T_2 values obtained at 17.6 T, and the reported literature chemical shift values from spectra obtained at 11.7 T. Due to much lower sensitivity, it was not possible to perform relaxation experiments for most of the samples at 4.7 T. However, the relatively rigid lattice in these minerals should result in field independent T_2 relaxation. The measured T_2 values for CaS (Table 3, column 5) are consistent with this assumption. Because the spectra obtained in this study have line widths that are approximately 10-fold narrower than those obtained earlier, a better estimation of the isotropic chemical shift was achieved. Larger differences in chemical shifts (e.g. PbS) between this work and literature values are most likely sample dependent. Eckert and Yesinowski [16] showed that samples with different crystal forms had different chemical shifts. The chemical shifts of ZnS and PbS follow a bond orbital model developed by Harrison and co-workers [27,28], as shown in [16]. The chemical shifts of MgS, CaS, SrS, and BaS are described by the extended Kondo–Yamashita [29] approach which includes nearest neighbor interactions, also shown in [16].

Table 2
Summary of ^{33}S NMR line width data

Compound	$\nu_{1/2}$ (Hz)[a]@ 11.7 T Static	$\nu_{1/2}$(Hz) @ 4.7 T Static	$\nu_{1/2}$ (Hz) at 17.6 T Static	$\nu_{1/2}$ (Hz) at 4.7 T MAS = 6 kHz	$\nu_{1/2}$ (Hz) at 17.6 T MAS = 6 kHz
Li_2S	1380	—[e]	850	70	65
Na_2S	500	360	580	30	40
MgS	300	90	290	30	35
CaS	100	55	200	4	12
ZnS	800[b]	1200	900	300	130
SrS	100	100	230	20	50
PbS	580[c] 300[d]	250	580	170	340
BaS	250	75	260	65	110

[a] Data obtained from [16].
[b] Mineral sample sphalerite, 1% Fe, from Picher, Oklahoma.
[c] Mineral sample galena from Picher, Oklahoma.
[d] Mineral sample galena from Kansas.
[e] Signal too weak.

Table 3
Summary of chemical shifts and T_1 and T_2 relaxation measurements

Compound	δ (ppm)[a] 11.74 T	δ (ppm) 17.6 T	T_1 (s) 17.6 T MAS = 6 kHz	T_2 (ms) @ 17.6 T MAS = 6 kHz
Li_2S	−347	−343.9	37 ± 2	11 ± 1
Na_2S	−338	−339.5	19.2 ± 0.3	43 ± 5
MgS	−174	−174.9	19 ± 2	340 ± 30
CaS	−28.5	−29.1	31 ± 5	4600 ± 500 4400 ± 700[f]
ZnS	−228[b] −231[c]	−236.5	11 ± 1	600 ± 200
SrS	42.8	43.5	20 ± 1	720 ± 230
PbS	−297[d] − 293[e]	−292.4	1.4 ± 0.1	25 ± 5
BaS	291	291.3	9 ± 1	200 ± 100

[a] Data obtained from [16].
[b] Mineral sample sphalerite, 1% Fe, Picher, Oklahoma.
[c] From MCB.
[d] Mineral sample galena from Picher, Oklahoma.
[e] Mineral sample galena from Kansas.
[f] Value measured at 4.7 T. Chemical shifts are referenced relative to external 1 M aqueous Cs_2SO_4 (pH 7.5) at 333 ppm from CS_2.

Spin lattice relaxation measurements were obtained for the first time for ^{33}S at 17.6 T. In general, the larger the line width the shorter the spin lattice relaxation time.

As discussed above, multiple factors contribute to the observed line width. These factors have varying relative importance depending on the specific compound, the field strength, and the spectral acquisition conditions (i.e., static or MAS). In order to quantitatively sort the relative importance of these contributions to the observed line width, we have obtained spectra at two field strengths under a variety of conditions. At two field strengths the static line width at half height ($\Delta\nu_{1/2}^{17.6\mathrm{T}}$ and $\Delta\nu_{1/2}^{4.7\mathrm{T}}$) can be given by

$$\Delta\nu_{1/2}^{17.6\,\mathrm{T}} = \Delta\nu_{\mathrm{QCC}} + \Delta\nu_{\mathrm{CSD}} + \Delta\nu_{T_2} + \Delta\nu_{\mathrm{CSA}} + \Delta\nu_{\mathrm{D}}, \quad (2)$$

$$\Delta\nu_{1/2}^{4.7\,\mathrm{T}} = \Delta\nu'_{\mathrm{QCC}} + \Delta\nu'_{\mathrm{CSD}} + \Delta\nu_{T_2} + \Delta\nu'_{\mathrm{CSA}} + \Delta\nu'_{\mathrm{D}}, \quad (3)$$

where $\Delta\nu_{1/2}$ denotes the line width contribution from quadruple coupling ($\Delta\nu_{\mathrm{QCC}}$), chemical shift dispersion ($\Delta\nu_{\mathrm{CSD}}$), transverse relaxation ($\Delta\nu_{T_2}$), chemical shift anisotropy ($\Delta\nu_{\mathrm{CSA}}$), and dipolar coupling (Δ_{D}). The dipolar coupling and T_2 are expected to be field independent. However, field-dependent contributions are possible for the other components. For a sample spinning at the magic angle at a frequency greater than the static line width, Eqs. (2) and (3) reduce to Eqs. (4) and (5).

$$\Delta\nu_{1/2}^{17.6\,\mathrm{T}} = \Delta\nu_{\mathrm{QCC}} + \Delta\nu_{\mathrm{CSD}} + \Delta\nu_{T_2}, \quad (4)$$

$$\Delta\nu_{1/2}^{4.7\,\mathrm{T}} = \Delta\nu'_{\mathrm{QCC}} + \Delta\nu'_{\mathrm{CSD}} + \Delta\nu_{T_2}, \quad (5)$$

In Eqs. (4) and (5), $\Delta\nu_{T_2}$ can be measured independently, leaving two equations with two unknowns. Table 4 summarizes the magnitude of the various contributions to the observed MAS line width at 4.7 and 17.6 T. It shows that T_2 relaxation only contributes significantly as a line broadening mechanism for Li_2S, Na_2S, and to a small degree for ^{207}Pb. Furthermore, it reveals that CSD plays a substantial role in defining the spectral line width in the remaining sulfides except ZnS. In ZnS, QCC is the major line broadening mechanism.

One would expect the T_1 and T_2 relaxation values to parallel QCC contributions to the line width if quadrupolar interactions are the predominant mechanism for T_1 and T_2 relaxation. However, these correlations are not observed. Comparison of $\Delta\nu_{\mathrm{QCC}}$ (Table 4, column 3)

Table 4
Magnitude of the various contributions to the observed MAS line width at 4.7 and 17.6 T

Compound	Contribution to observed line width			
	$\Delta\nu_{1/2}$ (Hz) 4.7T/17.6 T	$\Delta\nu_{\mathrm{QCC}}$ (Hz) 4.7/17.6 T	$\Delta\nu_{\mathrm{CSD}}$ (Hz) 4.7/17.6 T	$\Delta\nu_{T_2}$ (Hz)17.6 T
Li_2S	70/65	34/9	7/27	29
Na_2S	30/40	15/4	8/29	7
MgS	30/35	22/6	8/29	<1
CaS	4/12	0/0	3/11	<1
ZnS	300/130	285/76	14/53	<1
SrS	20/50	7/2	13/48	<1
PbS	170/340	75/20	82/307	13
BaS	65/110	37/10	26/98	2

with T_1 (Table 3, column 4) reveals that the $\Delta\nu_{QCC}$ varies over a range from 0 to 76 Hz while most of the T_1 values are in the range of 10–30 s. Comparison of $\Delta\nu_{QCC}$ with T_2 values shows that ZnS, which has a relatively large $\Delta\nu_{QCC}$, has a long T_2. At the same time Li_2S, Na_2S, and PbS which have relatively small $\Delta\nu_{QCC}$ values, have the shortest T_2 values. T_2's for the remaining samples are 10–100-fold greater. These data are consistent with the predominant contribution to T_2 relaxation coming from dipole–dipole interactions between sulfur and adjacent metal ions. ^{7}Li, ^{23}Na, and ^{207}Pb have a relatively high natural abundance 93, 100, and 23%, respectively. In addition, they all have relatively high gyromagnetic ratios. The NMR active isotopes of the remaining metals have very low natural abundances and/or very low gyromagnetic ratios, minimizing the effects of dipole–dipole interactions with ^{33}S.

4. Conclusions

This work shows the dramatic improvements in resolution that can be obtained by just spinning the sample at the magic angle. In view of the fact that QCC was relatively small in these samples, the use of a very high magnetic field strength is not essential to achieve significant line narrowing in these inorganic sulfides. However, the higher sensitivity and the reduced probe ringing at 17.6 T does result in simplified data collection, better quality spectra, and dramatic improvements in sensitivity. It was shown that for most of the samples CSD was the primary factor influencing line width. Unlike almost all other sulfur containing materials it is relatively easy to obtain good spectra of metal sulfides and to extract useful chemical shift information.

Acknowledgments

We thank Ann Bolek for her efforts in obtaining much of the crystal structure literature, and Simon Stakleff for his work to maintain the NMR equipment used. We acknowledge the Kresge Foundation, the donors to the Kresge Challenge Program at the University of Akron for funds to purchase the NMR instruments used in this work, and partial support of this research by the Petroleum Research Fund administered by the American Chemical Society (26776-AC).

References

[1] S.S. Dharmatti, H.E. Weaver, Magnetic moment of sulfur-33, Phys. Rev. 83 (1951) 845.
[2] V.M. Bzhezovsky, G.A. Kalabin, Chemistry of Organosulfur Compounds, Horwood, Chichester, 1990.
[3] J.F. Hinton, Sulfur-33 NMR spectroscopy, A. Rep. NMR Spectrosc. 19 (1987) 1–34.
[4] P.S. Belton, I.J. Cox, R.K. Harris, Experimental sulfur-33 nuclear magnetic resonance spectroscopy, J. Chem. Soc., Faraday Trans. 2 81 (1985) 63.
[5] G. Barbarella, Sulfur-33 NMR, Prog. NMR Spectrosc. 25 (1993) 317.
[6] C. Brevard, P. Granger, Handbook of High Resolution Multinuclear NMR, Wiley, New York, 1981.
[7] G. Maciel, High-resolution nuclear magnetic resonance of solids, Science 226 (1984) 282.
[8] G.C. Chingas, K.T. Mueller, A. Pines, J. Stebbins, Y. Wu, J.W. Zwanziger, Dynamic-angle spinning of quadrupolar nuclei, J. Magn. Reson. 86 (1990) 470.
[9] S. Ganapathy, S. Schramm, E. Oldfield, Variable-angle sample-spinning high resolution NMR of solids, J. Chem. Phys. 77 (1982) 4360.
[10] E. Oldfield, R.J. Kirkpatrick, High-resolution nuclear magnetic resonance of inorganic solids, Science 227 (1985) 1537.
[11] K.T. Mueller, B.Q. Sun, G.C. Chingas, J.W. Zwanziger, T. Terao, A. Pines, Dynamic-angle spinning of quadrupolar nuclei, J. Magn. Reson. 86 (1990) 470.
[12] A. Samoson, A. Pines, Double rotor for solid-state NMR, Rev. Sci. Instrum. 60 (1989) 3239.
[13] E.W. Wooten, K.T. Mueller, A. Pines, New angles in nuclear magnetic resonance sample spinning, Acct. Chem. Res. 25 (1992) 209.
[14] L. Frydman, J.S. Harwood, Isotropic spectra of half-integer quadrupolar spins from bidimensional magic-angle spinning NMR, J. Am. Chem. Soc. 117 (1995) 5367.
[15] A. Medek, J.S. Harwood, L. Frydman, Multiple-quantum magic-angle spinning NMR: a new method for the study of quadrupolar nuclei in solids, J. Am. Chem. Soc. 117 (1995) 12779.
[16] H. Eckert, J.P. Yesinowski, Sulfur-33 NMR at natural abundance in solids, J. Am. Chem. Soc. 108 (1986) 2140.
[17] T.J. Bastow, NMR study of the II–VI semiconductors ZnX (X = O, S, Se, Te), Mater. Australas. 19 (1987) 12.
[18] T.J. Bastow, S.N. Stuart, NMR study of the zinc chalcogenides (ZnX, X = O, S, Se, Te), Phys. Status Sol. B 145 (1988) 719.
[19] W.H. Press, B.P. Flannery, S.A. Teukolsky, W.T. Vettering, Numerical Recipes in C: The Art of Scientific Computing, Cambridge University Press, Cambridge, 1988.
[20] J. Skibsted, N.C. Nielsen, H. Bildsøe, H.J. Jakobsen, Satellite transitions in MAS NMR spectra of quadrupolar nuclei, J. Magn. Reson. 95 (1991) 88.
[21] J. Skibsted, N.C. Nielsen, H. Bildsøe, H.J. Jakobsen, Vanadium-51 MAS NMR spectroscopy: determination of quadrupole and anisotropic shielding tensors, including the relative orientation of their principal-axis systems, Chem. Phys. Lett. 188 (1992) 405.
[22] J. Skibsted, N.C. Nielsen, H. Bildsøe, H.J. Jakobsen, Magnitudes and relative orientation of vanadium-51 quadrupole coupling and anisotropic shielding tensors in metavanadates and potassium vanadium oxide (KV_3O_8) from vanadium-51 MAS NMR spectra. Sodium-23 quadrupole coupling parameters for a- and b-$NaVO_3$, J. Am. Chem. Soc. 115 (1993) 7351.
[23] W.A. Daunch, P.L. Rinaldi, Natural-abundance solid state ^{33}S NMR with high-speed magic-angle spinning, J. Magn. Reson. A 123 (A) (1996) 219.
[24] A.P.M. Kentgens, A practical guide to solid-state NMR of half-integer quadrupolar nuclei with some applications to disordered systems, Geoderma 80 (1997) 271.
[25] T.C. Farrar, E.D. Becker, Pulse and Fourier Transform NMR, Academic Press, New York, 1971.
[26] G. Neue, C. Dybowski, M.L. Smith, M.A. Hepp, D.L. Perry, Determination of $^{207}Pb^{2+}$ chemical shift tensors from precise powder lineshape analysis, Solid State NMR 6 (1996) 241.
[27] W.A. Harrison, Bond-orbital model and the properties of tetrahedrally coordinated solids, Phys. Rev. B 8 (1973) 4487.

[28] W.A. Harrison, S. Ciraci, Bond-orbital model. II, Phys. Rev. B 10 (1974) 1516.
[29] J. Kondo, J. Yamashita, Nuclear quadrupolar relaxation in ionic crystals, J. Phys. Chem. Solids 10 (1959) 245.
[30] F. Kubel, B. Bertheville, H. Bill, Crystal structure of dilithium-sulfide, Li_2S, Zeitschrift fuer Kristallographie—New Crystal Struct. 214 (3) (1999) 302.
[31] A. Claassen, The crystal structure of the anhydrous alkali monosulphides. I, Recueil des travaux chimiques des Pays-Bas. 44 (1925) 790.
[32] E. Zintl, A. Harder, B. Dauth, Lattice structure of the oxides, sulfides, selenides and tellurides of lithium, sodium and potassium, Z. Elektrochem. 40 (1934) 588.
[33] M. Kizilyalli, M. Bilgin, H. Kizilyalli, Solid-state synthesis and X-ray diffraction studies of sodium sulfide (Na_2S), J. Solid State Chem. 85 (2) (1990) 283.
[34] W. Primak, H. Kaufman, R. Ward, X-ray diffraction studies of systems involved in the preparation of alkaline earth sulfide and selenide phosphors, J. Am. Chem. Soc. 70 (1948) 2043.
[35] S. Holgersson, Die Struktur der Sulfide von Mg, Ca, Sr und Ba, Z. Anorg. Chem. 126 (1923) 179.
[36] Y. Kaneko, K. Morimoto, K. Takao, Optical properties of alkaline-earth chalcogenides. I. Single crystal growth and infrared reflection spectra due to optical phonons, J. Phys. Soc. Jpn. 51 (7) (1982) 2247.
[37] P. Wu, R. Kershaw, K. Dwight, A. Wold, Growth and characterization of nickel-doped ZnS single crystals, Mater. Res. Bull. 24 (1989) 49.
[38] Y.R. Do, R. Kershaw, K. Dwight, A. Wold, The crystal growth and characterization of the solid solutions $(ZnS)_{1-X}(CuGaS_2)_X$, J. Solid State Chem. 96 (1992) 360.
[39] H. Cui, R.D. Pike, R. Kershaw, K. Dwight, A. Wold, Syntheses of Ni3S2, Co9S8, and ZnS by the decomposition of diethyldithiocarbamate complexes, J. Solid State Chem. 101 (1992) 115.
[40] M.T. Sebastian, D. Pandey, P. Krishna, X-ray diffraction study of the 2H to 3C solid state transformation in vapour grown single crystals of ZnS, Phys. Stat. Sol. A 71 (1982) 633.
[41] A.R. Verma, P. Krishna, Polymorphism and Polytypism in Crystals, Wiley, New York, 1966.
[42] K. Syassen, Pressure-induced structural transition in SrS, Phys. Stat. Sol. A 91 (1985) 11.
[43] I.P. Parkin, A.T. Rowley, Metathesis routes to tin and lead chalcogenides, Polyhedron 12 (24) (1993) 2961.
[44] Y. Noda, S. Ohba, S. Sato, Y. Saito, Charge distribution and atomic thermal vibration in lead chalcogenide crystals, Acta Cryst. B 39 (1983) 312.
[45] Y. Noda, K. Masumoto, S. Ohba, Y. Saito, K. Toriumi, Y. Iwata, I. Shibuya, Temperature dependence of atomic thermal parameters of lead chalcogenides, PbS, PbSe, and PbTe, Acta Cryst. C 43 (1987) 1443.
[46] T. Chattopadhyay, H.G. von Schnering, W.A. Grosshans, W.B. Holzapfel, High pressure synchrotron radiation, Physica B 139–140 (1986) 356.
[47] S.T. Weir, Y.K. Vohra, A.L. Ruoff, High-pressure phase transitions and the equations of state of Bas and BaO, Phys. Rev. B 33 (6) (1986) 4221.